Rapid Summation of the Green's Function for the Rectangular Waveguide

Myun-Joo Park and Sangwook Nam

***Abstract*— A rapid calculation scheme is proposed for the potential Green's functions in the rectangular waveguide. The Ewald sum technique converts the slowly convergent Green's function series into the sum of two rapidly convergent series through the error-function transformation. The efficient numerical calculation method of the resultant expression is also presented.**

***Index Terms*—Ewald sum, Green's function, rectangular waveguide.**

I. Introduction

In general, the method of moments (MoM) analysis of the rectangular-waveguide problems calls for some specialized methods to accelerate the slowly convergent Green's function [1], [2]. As is well known, the two-dimensional infinite series representing the rectangular-waveguide Green's function has very poor convergence property when the source and observation points are located closely to each other along the axis of the waveguide. The origin of this convergence problem can be traced back to that of the free-space periodic Green's function, for which several effective methods have been proposed based on the combined spatial–spectral-domain hybrid-calculation schemes [3].

The Ewald sum technique is a powerful method for various periodic problems [4], [5] and it has also been applied to the rectangular-cavity problems [6]. In this paper, a rapid calculation scheme is proposed for the potential Green's functions of the rectangular waveguide based on the Ewald sum technique. The proposed method converts the Green's function into the sum of the spatial and spectral series. Since all terms of the two series are weighted by the fast-decaying error function, they are both exponentially convergent, and the Green's function can be calculated accurately with only a small number of terms in the series. In addition, several effective calculation methods are devised for the rapid numerical evaluation of the resultant expressions, which results in further computational savings in the practical implementation of the proposed method.

II. Theory

The potential Green's functions for the rectangular waveguide can be written as the diagonal dyad [1]. Each component of the Green's dyad can be expressed in two different forms, one is the modal series in the spectral domain and the other is the image series in the spatial domain. The two following forms are given explicitly for the $\hat{x}\hat{x}$ component of the magnetic-vector potential Green's function:

$$\begin{aligned}
G_{xx}^{A} &= \frac{\mu}{2ab}\sum_{m,n=0}^{\infty}\frac{\varepsilon_m\varepsilon_n}{\gamma_{mn}}\exp\left(-\gamma_{mn}|z-z'|\right)\cos\frac{m\pi x}{a}\\
&\quad\cdot\cos\frac{m\pi x'}{a}\times\sin\frac{n\pi y}{b}\sin\frac{n\pi y'}{b}\\
\varepsilon_i &= \begin{cases}1, & i=0\\ 2, & i\neq 0\end{cases}\\
\gamma_{mn}^2 &= (m\pi/a)^2+(n\pi/b)^2-k^2
\end{aligned}\tag{1}$$

Manuscript received November 14, 1997; revised August 9, 1998.

The authors are with the School of Electrical Engineering, Seoul National University, Seoul 151-742, Korea.

Publisher Item Identifier S 0018-9480(98)09059-0.

$$\begin{aligned}
G_{xx}^{A} &= \frac{\mu}{4\pi}\sum_{m,n=-\infty}^{\infty}\sum_{i=0}^{3}A_i^{xx}\frac{\exp\left(-jkR_{i,mn}\right)}{R_{i,mn}}\\
A_i^{xx} &= \begin{cases}+1, & i=0,2\\ -1, & i=1,3\end{cases}\\
R_{i,mn} &= \sqrt{(X_i+2ma)^2+(Y_i+2nb)^2+(z-z')^2}\\
X_i &= \begin{cases}x-x', & i=0,1\\ x+x', & i=2,3\end{cases}\\
Y_i &= \begin{cases}y-y', & i=0,2\\ y+y', & i=1,3\end{cases}
\end{aligned}\tag{2}$$

where a, b are the waveguide dimensions in x, y directions, respectively, and k is the wavenumber.

According to the Ewald sum method [4], [5], the above Green's function can be divided into two parts as follows:

$$G_{xx}^{A} = G_{xx1}^{A}+G_{xx2}^{A}\tag{3}$$

$$\begin{aligned}
G_{xx1}^{A} &= \frac{\mu}{8ab}\sum_{m,n=0}^{\infty}\frac{\varepsilon_m\varepsilon_n}{\sqrt{\pi}}\int_{1/E}^{\infty}\\
&\quad\cdot\exp\left\{-\frac{\gamma_{mn}^2s^2}{4}-\frac{(z-z')^2}{s^2}\right\}ds\times\cos\frac{m\pi x}{a}\\
&\quad\cdot\cos\frac{m\pi x'}{a}\sin\frac{n\pi y}{b}\sin\frac{n\pi y'}{b}
\end{aligned}\tag{3a}$$

$$G_{xx2}^{A} = \frac{\mu}{2\pi}\sum_{m,n=-\infty}^{\infty}\sum_{i=0}^{3}\frac{A_i^{xx}}{\sqrt{\pi}}\int_{0}^{E}\exp\left(-R_{i,mn}^2s^2+\frac{k^2}{4s^2}\right)ds\tag{3b}$$

where E is an adjustable parameter in the Ewald sum method.

The integrals in (3) can be evaluated in terms of the complementary error function [4], [5], with the following results:

$$\begin{aligned}
G_{xx1}^{A} &= \frac{\mu}{4ab}\sum_{m,n=0}^{\infty}\frac{\varepsilon_m\varepsilon_n}{\gamma_{mn}}f(|z-z'|,\gamma_{mn},E)\\
&\quad\times\cos\frac{m\pi x}{a}\cos\frac{m\pi x'}{a}\sin\frac{n\pi y}{b}\sin\frac{n\pi y'}{b}\\
f(|z-z'|,&\gamma_{mn},E)\\
&\equiv\exp\left\{\gamma_{mn}(z-z')\right\}\operatorname{erfc}\left\{\gamma_{mn}/2E+(z-z')E\right\}\\
&\quad+\exp\left\{-\gamma_{mn}(z-z')\right\}\operatorname{erfc}\left\{\gamma_{mn}/2E-(z-z')E\right\}
\end{aligned}\tag{4}$$

$$\begin{aligned}
G_{xx2}^{A} &= \frac{\mu}{8\pi}\sum_{m,n=-\infty}^{\infty}\sum_{i=0}^{3}A_i^{xx}\frac{1}{R_{i,mn}}\\
&\quad\cdot\left\{\exp\left(-jkR_{i,mn}\right)\operatorname{erfc}\left(R_{i,mn}E-jk/2E\right)\right.\\
&\quad\left.+\exp\left(jkR_{i,mn}\right)\operatorname{erfc}\left(R_{i,mn}E+jk/2E\right)\right\}.
\end{aligned}\tag{5}$$

Loosely speaking, the G_{xx1}^{A} and the G_{xx2}^{A} series correspond to the modal and image expansion of the waveguide Green's function, respectively, with each term of the series weighted by the complementary error function. Since the complementary error function $\operatorname{erfc}(z)$ behaves asymptotically as $\exp(-z^2)/\sqrt{\pi}z$, the above two series are both rapidly convergent.

In many practical situations, the medium inside the waveguide is lossless, and then, the above expressions can be simplified further to reduce the computational burden. In that case, the wavenumber k becomes real and the G_{xx2}^{A} series can be reduced to the following form using the complex conjugate property of the error function [6],

[7]:

$$G^A_{xx2} = \frac{\mu}{4\pi}\sum_{m,n=-\infty}^{\infty}\sum_{i=0}^{3}A_i^{xx}\frac{1}{R_{i,mn}} \cdot \mathrm{Re}\left[\exp\left(-jkR_{i,mn}\right)\mathrm{erfc}\left(R_{i,mn}E - jk/2E\right)\right] \quad (6)$$

where $\mathrm{Re}[A]$ designates the real part of a complex number A. Similarly, the following simplified form can be used for the propagating mode terms of the G^A_{xx1} series:

$$f(|z-z'|,\gamma_{mn},E) = 2\exp\left\{-jk_{zmn}(z-z')\right\} + j2 \cdot \mathrm{Im}\left[\exp\left\{jk_{zmn}(z-z')\right\} \cdot \mathrm{erfc}\left\{jk_{zmn}/2E + (z-z')E\right\}\right]$$
$$k_{zmn} = j\sqrt{-\gamma_{mn}^2}, \quad \gamma_{mn}^2 < 0 \quad (7)$$

where $\mathrm{Im}[A]$ denotes the imaginary part of a complex number A. As a result of the above simplifications, the total number of complex error-function evaluation is reduced by the factor of two. Furthermore, novel methods have been developed for the efficient numerical calculation of these reduced forms, which are given below.

In general, the numerical calculation of the error functions with complex argument requires a considerable amount of computation time. However, a careful examination of the above reduced forms reveals that the complex error functions appear in one of the following two forms in the present method:

$$\mathrm{Re}\left\{\exp\left(-jkR\right)\mathrm{erfc}\left(RE - jk/2E\right)\right\} = \mathrm{Re}\left\{\exp\left(-j2xy\right)\mathrm{erfc}\left(x - jy\right)\right\}, \qquad x = RE, \quad y = k/2E \quad (8)$$

$$\mathrm{Im}\left[\exp\left\{jk_z(z-z')\right\}\mathrm{erfc}\left\{jk_z/2E + (z-z')E\right\}\right] = \mathrm{Im}\left\{\exp\left(j2xy\right)\mathrm{erfc}\left(x + jy\right)\right\}, \qquad x = (z-z')E, \quad y = k_z/2E. \quad (9)$$

The above compound forms can be calculated effectively using the following series expansions derived from the infinite series approximation of the complex error function [7, eq. (7.1.29)]:

$$\mathrm{Re}\left\{\exp\left(-j2xy\right)\mathrm{erfc}\left(x - jy\right)\right\} = \mathrm{erfc}\left(x\right)\cos\left(2xy\right) + \frac{4x}{\pi}\exp\left(-x^2\right) \cdot \sum_{n=1}^{\infty}\frac{\exp\left(-n^2/4\right)}{n^2+4x^2}\left(\cosh\left(ny\right) - \cos\left(2xy\right)\right) + \frac{\exp\left(-x^2\right)}{2\pi x}\left(1-\cos\left(2xy\right)\right) + \varepsilon(x,y) \quad (10)$$

$$\mathrm{Im}\left\{\exp\left(j2xy\right)\mathrm{erfc}\left(x + jy\right)\right\} = \mathrm{erfc}\left(x\right)\sin\left(2xy\right) - \frac{2}{\pi}\exp\left(-x^2\right)\sum_{n=1}^{\infty}\frac{\exp\left(-n^2/4\right)}{n^2+4x^2} \cdot \left(n\sinh\left(ny\right) + 2x\sin\left(2xy\right)\right) - \frac{\exp\left(-x^2\right)}{2\pi x} \cdot \sin\left(2xy\right) + \varepsilon(x,y). \quad (11)$$

In the case of the real error function, various aproximation formulas are available for its effective numerical calculation [7].

III. Numerical Result

The proposed method has been applied to the standard X-band waveguide WR90 ($a = 2.186$ cm, $b = 1.016$ cm).

Fig. 1 shows the typical convergence behavior for the $\hat{x}\hat{x}$ component of the magnetic-vector potential Green's function in modal expansion (1). As the axial distance between the source and observation point gets closer, the convergence of the Green's function becomes worse, and it does not seem to converge at all when the two points are on the same cross-sectional plane in the waveguide ($z = z'$). The situation is even worse for the image expansion of the Green's function, and no convergence have been obtained numerically for the three cases treated in Fig. 1.

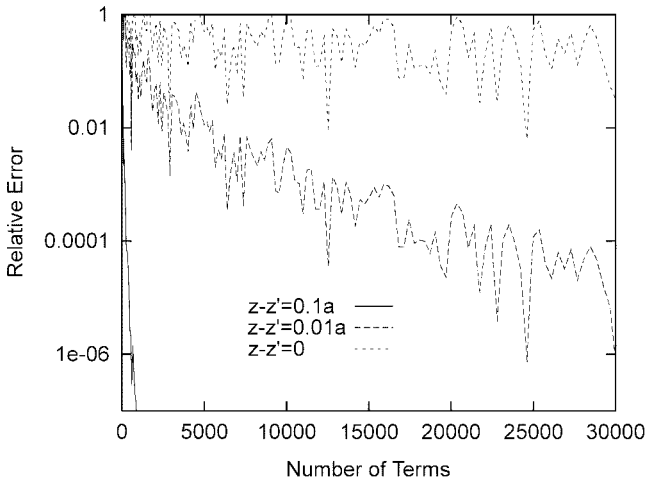

Fig. 1. Typical convergence behavior of the Green's function (G^A_{xx}) in modal expansion ($x' = 0.5a$, $y' = 0.5b$, $x = 0.1a$, $y = 0.1b$).

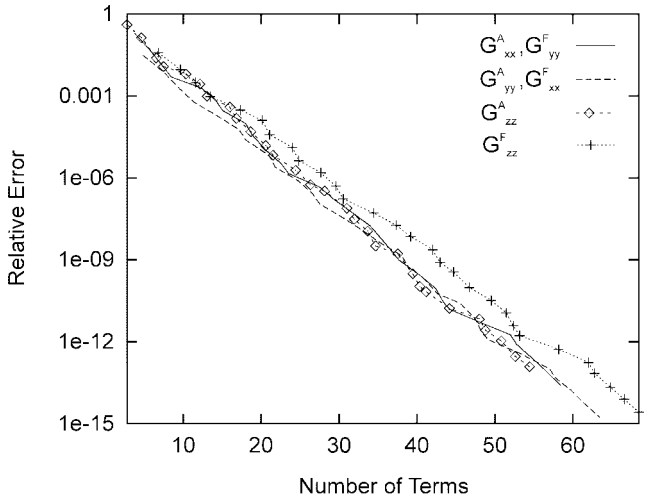

Fig. 2. Average convergence behavior of the Ewald sum method.

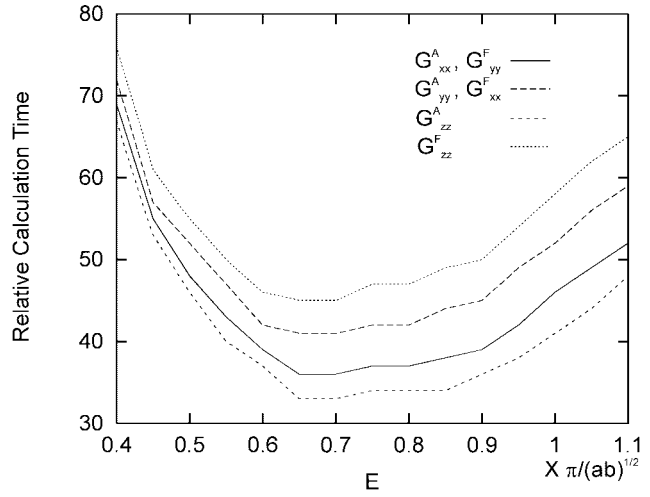

Fig. 3. Change of the calculation time with variation of the Ewald sum parameter E.

Fig. 1 shows the typical convergence behavior for the $\hat{x}\hat{x}$ component of the magnetic-vector potential Green's function in modal expansion (1). As the axial distance between the source and observation point gets closer, the convergence of the Green's function becomes worse, and it does not seem to converge at all when the

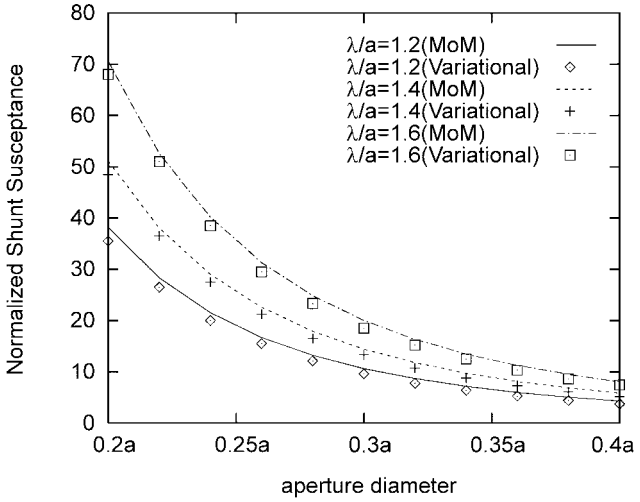

Fig. 4. Normalized susceptance of the centered circular aperture in the cross-sectional plane of a rectangular waveguide (λ: wavelength).

In comparison, the Ewald sum-based calculations presented in Fig. 2 show very rapid convergence. The average error decreases exponentially as the number of calculated terms increases. In Fig. 2, superscripts A and F desiginates the magnetic- and electric-vector potential functions, respectively. The results shown in this figure have been obtained through averaging Green's function calculations over 625 different source–observation point pairs (25 source points $\times$ 25 observation points) evenly distributed on the same cross-sectional plane of the waveguide ($z = z'$). On average, 18.73 and 22.01 terms were needed to obtain 10^{-4} and 10^{-5} convergence, respectively. Therefore, the proposed method can achieve sufficient accuracy for most numerical applications with only about 20 term calculations.

The next result concerns the optimum choice of the Ewald sum parameter E. In Fig. 3, relative calculation times are given as a function of the parameter E. For the small and large values of E, the total calculation time increases due to the slow convergence of the spatial and spectral series, respectively. The overall average calculation time is minimized for the E values in the range of $0.6\pi/\sqrt{ab} - 0.9\pi/\sqrt{ab}$ under the proposed calculation schemes.

Finally, Fig. 4 shows the application of the proposed method to the scattering analysis of a centered circular aperture in the cross-sectional plane of the rectangular waveguide [8]. The MoM analysis employed the Galerkin's method with triangular-rooftop basis functions. The aperture has been discretized with 90 triangular elements and 145 basis functions. It took about 30 s to obtain one point data on a Sun UltraSpark1 workstation. The calculated results agree well with those by the variational method [8] within the error bound of the variational formula.

REFERENCES

[1] B. C. Ahn, "Moment method analysis of a narrow wall inclined slot on a rectangular waveguide," Ph.D. dissertation, Dept. Elect. Eng., Univ. Mississippi, Oxford, 1992.

[2] J. Xu, "Fast convergent dyadic Green's function in a rectangular waveguide," *Int. J. Infrared Millim. Waves*, vol. 30, no. 3, pp. 409–418, May. 1993.

[3] R. E. Jorgenson and R. Mittra, "Efficient calculation of the free-space periodic Green's function," *IEEE Trans. Antennas Propagat.*, vol. 38, pp. 633–642, May 1990.

[4] P. P. Ewald, "Die berechnung optischer und elektrostatischen gitterpotentiale," *Ann. Phys.*, vol. 64, pp. 253–268, 1921.

[5] K. E. Jordan, G. R. Richter, and P. Sheng, "An efficient numerical evaluation of the Green's function for the Helmholtz operator on periodic structures," *J. Comput. Phys.*, vol. 63, no. 16, pp. 222–235, 1986.

[6] M.-J. Park, J. Park, and S. Nam, "Efficient calculation of the Green's function for the rectangular cavity," *IEEE Microwave Guided Wave Lett.*, vol. 8, pp. 124–126, Mar. 1998.

[7] M. Abramowitz and I. Stegun, Eds., *Handbook of Mathematical Functions*. New York: Dover, 1970.

[8] N. Marcuvitz, *Waveguide Handbook*. New York: McGraw-Hill, 1951.

FDTD Improvement by Dielectric Subgrid Resolution

Gaetano Marrocco, Marco Sabbadini, and Fernando Bardati

***Abstract*— Material inhomogeneities are taken into account in the standard finite–difference time-domain method by staircase modeling of medium boundaries. Resolution is, therefore, limited by Yee's cell sizes. In this paper, a new scheme is proposed, which improves material resolution without increasing the demand of computer resources.**

***Index Terms*—Dielectric inhomogeneity, FDTD method, subgridding.**

I. INTRODUCTION

The finite-difference time-domain (FDTD) method [1] is well suited to compute electromagnetic-field components, which are tangential to the interface among different dielectric media. Dielectric discontinuities are modeled by plane surfaces through mesh nodal points while each elementary cell is homogeneously filled. To analyze complicated structures, such as irregularly shaped and inhomogeneous microwave devices, it is necessary to use a fine cell size and large computer resources. Moreover, the modeling of curvilinear boundaries [see Fig. 1(a)] requires staircase approximation in order to accommodate the structure to the computational grid. In such a case, the accuracy is related to grid-size refinement, i.e., to computer resources. Halving the cell size improves boundary accommodation [see Fig. 1(b)]. More economical in terms of computational burden, an inhomogeneous cell can be treated as it was homogeneously filled by a medium with parameters ε, σ, μ, which are obtained by volume averaging of the different media inside the cell. However, this method does not give very accurate results. Alternative formulations have been proposed, which model boundaries by local modification of Maxwell's equations [2]–[4], local grid modification [5], or globally irregular gridding [6], [7]. These methods differ substantially in the modeling of dielectric interfaces and generally require complex algorithms and preprocessing. A different method by Gwarek [8], [9] is based on separate modeling of several kinds of dielectric discontinuities, which may occur when a standard FDTD cell is intersected by a dielectric interface [see Fig. 1(c)]. In this method, a couple of effective parameters is associated to each intersection,

Manuscript received March 10, 1997; revised August 12, 1998.

G. Marrocco and F. Bardati are with DISP, University of Rome "Tor Vergata," 00133 Rome, Italy.

M. Sabbadini is with ESA-ESTEC, AG 2200 Noordwijk, The Netherlands.

Publisher Item Identifier S 0018-9480(98)09063-2.